The fate of continuous input of relatively heavy fluid at the base of a porous medium

Herbert E. Huppert[1,2,3,4]†, R.S.J. Sparks[4], S.S. Pegler[1] and A. Rust[4]

[1]Institute of Theoretical Geophysics, Department of Applied Mathematics and Theoretical Physics, University of Cambridge, CB3 0WA, UK

[2]Faculty of Science, University of Bristol, BS8 1RJ, UK

[3]School of Mathematics and Statistics, University of New South Wales, Sydney, NSW, 2052 Australia

[4]Department of Earth Sciences, University of Bristol, BS8 1RJ, UK

(Received ?; revised ?; accepted ?. - To be entered by editorial office)

18 July 2017
Co-authors, how exactly do you want your names?

We evaluate theoretically and confirm experimentally the shape of the fluid envelope resulting from the input of relatively heavy fluid at a constant rate from a point source at the base of a homogeneous porous medium. We determine that in three dimensions an initially expanding hemisphere transitions into a gravity current flowing over the assumed rigid, horizontal, impermeable bottom of the porous medium. We show that a range of increasing transition times occur if defined by extrapolation of the relationships in the two extreme regimes (hemispherical shape and by gravity current) so that they intersect for: the ratio of buoyancy to fluid resistance; the horizontal extent of the fluid; the ratio of height at the centre to the radius; and just the height at the centre. The study is also taken over to two-dimensional geometries. Experiments in a Hele Shaw cell agree well with the theoretical predictions. The results are extrapolated to consider flow in a two-layer system - in order to begin to understand effects due to a vertically heterogeneous pore structure. We sketch, and verify by experiment, that an expanding hemisphere in a lower layer can reach a much more permeable upper layer and flow as a gravity current - thereby uniting the two regimes.

1. Introduction

In many natural and industrial situations, relatively heavy fluid is continuously introduced at the base of a porous medium. The importance of this situation has lead to a whole series of laboratory experiments being undertaken to simulate such occurrences. Recently there has been an additional series of papers and laboratory experiments by authors from different groups motivated by the societally important problem of carbon sequestration, the final part of carbon capture and storage (CCS). To mitigate the effects of global warming, attributed to the current anthropogenic annual worldwide emission of 37 billion tonnes of carbon dioxide (CO_2), numerous groups around the world are evaluating how to store super-critical, liquid-like, CO_2 at depths in excess of 800m (roughly the depth associated with the pressure and temperature needed to compress CO_2 to the super-critical state). The CO_2 is relatively less dense than the surrounding, interstitial

† Email address for correspondence: heh1@damtp.cam.ac.uk

brine and so it rises like a buoyant plume until it encounters a relatively impermeable cap rock and spreads beneath it as a gravity current in a porous medium (see Huppert & Woods 1995, Bickle 2009 and Huppert & Neufeld 2014 and references therein for further information). Almost all the confirmatory laboratory experiments have employed the inverted situation of relatively heavy, salty water intruding into a porous medium with pure interstitial water to simulate the resulting flow.

There are situations in the Earth where dense fluids discharge into regions containing lower density interstitial fluids in permeable geological media. An important example occurs during discharges of high temperature fluids from magma chambers. These flows can cause discharges of gases at volcanoes and are associated with formation of metalliferous ore deposits. While the overall density of the fluids is less dense than surrounding ground waters they characteristically exsolve dense brines, which can separate and then displace surrounding fresh water in permeable crust.

One of our conclusions is that because the parameter values describing typical laboratory situations are very different from those describing realistic geological situations, the form of flow can be somewhat different. We demonstrate, both theoretically and experimentally, that the flow, assumed to issue from a point source at the base of a semi-infinite porous medium of constant permeability at constant rate Q, first spreads in the form of a hemisphere of steadily increasing radius [the radius $a(t) \propto t^{1/3}$ where t is time] with gravity, and hence the density difference between intruding and interstitial fluid, irrelevant, as is the viscosity of the fluids and permeability (rather than porosity) of the porous medium. A sketch of this and the subsequent flow make up figure 1. An ever increasing parameter we call the Alison number, $A(t)$, which reflects the importance of gravity and is a function of time, initially increases as $A(t) \propto t^{2/3}$, becoming comparable to unity at around $t/T = (18\pi\phi^3)^{-1/2}$, where T is the intrinsic time scale given by $T = (Q'/\beta^3)^{1/2}$ with $Q' = Q/\phi$, the buoyancy speed $\beta = \Delta\rho g k/(\phi\mu)$, where $\Delta\rho$ is the density difference between intruding and interstitial fluid, g the acceleration due to gravity, k the permeability, ϕ the porosity and μ the dynamic viscosity. Roughly around this time the flow transitions to a basal-hugging axisymmetric gravity current with radius $r_N(t) \propto t^{1/2}$, and height of the form $h(r,t) \propto f[r/r_N(t)]$ for some function $f(x) \approx (1-x)$, as has been well documented previously (Lyle et al. 2006). Thereafter $A(t)$ steadily continues to increase, but like $t^{1/2}$. Another important parameter is the mean slope of the intrusion, denoted by $\gamma(t)$, and defined by the ratio of the effective height over the input point $h(0,t)$ to the radius $a(t)\,[= h(0,t)$ initially and $r_N(t)$ finally]. Until the flow transitions to a gravity current $\gamma(t) = 1$, thereafter it approaches $\gamma = 0.58(t/T)^{-1/2}$.

Interestingly, using typical values for the laboratory $T \approx 1$ sec, far too short for the first regime to be easily seen. However, for some illustrative geological values of the parameters $(\Delta\rho/\rho \sim 0.1, \nu \sim 10^{-6} m^2 s^{-1}, \phi \sim 0.05, k \sim 10^{-15} m^2, Q \sim 10^{-5} m^3 s^{-1})\, t_a \sim 10^3$ yr, a rather different result. (More detailed figures are given in table 1).

We start in the next section by considering, in axisymmetric geometry, the initial response of an expanding hemisphere. We then recall the previously obtained solutions relevant to a gravity current obtained by Lyle et al. (2006) using D'Arcy's flow law (Bear 1972, Phillips 1991)

$$\nabla p = \mu \mathbf{u}/k - \rho \mathbf{g}, \tag{1.1}$$

where p is pressure and $\mathbf{g}$ the (vectorial) acceleration due to gravity. We show that the second term on the right-hand side of (1.1) is initially negligible and using just conservation of volume, we present the form of motion in the resultant hemisphere.

We define $A(t)$ to be the ratio of μ/k to ρg and evaluate its dependence on a suitably non-dimensional time for the two regimes. We determine where they intersect, denoted by

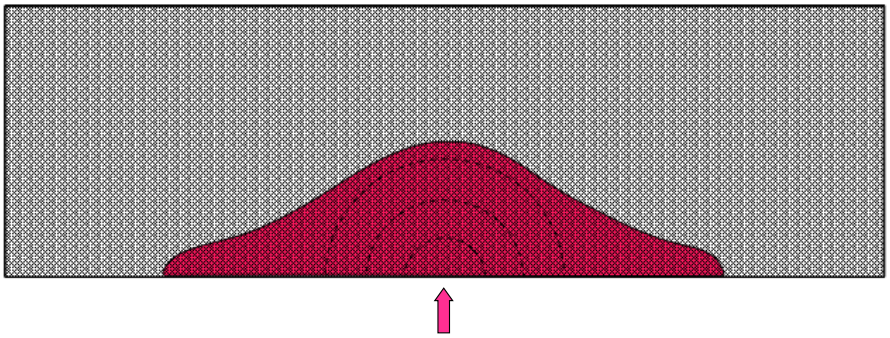

FIGURE 1. The typical responses to an input flux Q of heavy viscous fluid into a porous medium above an impermeable horizontal boundary. Initially the flow is in the form of a hemisphere (semi-circle for a two-dimensional situation) of radius $a(t)$ which transforms into a gravity current of horizontal extent $r_N(t)$ and height above the input of $h(0,t)$, where t is the time since initiation of the flow.

t_A. As far as this ratio is concerned, the flow is dominantly hemispherical for $t \ll t_A$ and dominantly a long, thin gravity current for $t \gg t_A$. We repeat this process to determine: t_a (based on the radius of the resulting flows; t_R (based on the height at centre) and t_γ (based on the ratio of height at the centre to radius - a proxy for the slope). We find that there is a wide disparity between these time scales. For the axisymmetric situation, in terms of a suitable timescale $T, t_A/T = 0.0081 < t_a/T = 0.094 < t_\gamma/T = 0.34 < t_h/T = 0.63$. For the two-dimensional case, in terms of a slightly differently defined timescale T_2, we find that $t_A/T_2 = 0.0043 < t_a/T_2 = 0.025 < t_\gamma/T_2 = 1.03 < t_h/T_2 = 38$.

We present numerical values of t_A, t_a, T_γ and t_h for typical parameters relevant to the laboratory, for which T is approximately 20s, and the field, for which T can be as large as 8500 years. We discuss, briefly, how to extend our results to flows in some vertically heterogeneous porous media, and present a somewhat dramatic experimental photo of how a relatively permeable upper layer can be a quite different flow regime from a relatively less permeable lower layer. We end the paper with a brief summary.

2. Hemispherical growth, $A(t) \ll 1$

Initially, as we have already stated and will demonstrate below, gravity is negligible. In a porous medium momentum effects are also negligible and there can be no difference between flow resistance in any direction. This is in complete contrast to the motion of high Reynolds number turbulent plumes (Morton, Taylor & Turner 1956), where a flux of relatively heavy fluid rises as a mainly vertically oriented, slowly expanding plume, to a height of $1.85 M_0^{3/4} F_0^{1/2}$, where M_0 is the momentum flux and F_0 the buoyancy flux at source, before falling back to the base to spread as a high Reynolds number, axisymmetric gravity current (Turner 1973, 1986, Simpson 1987, Ungarish 2009).

In the current case, conservation of volume dictates that

$$\frac{2}{3}\pi\phi a^3 = Qt \tag{2.1}$$

or

$$a(t) = \left(\frac{3Q'}{2\pi}\right)^{1/3} t^{1/3}, \tag{2.2}$$

where $Q' = Q/\phi$, from which it follows that

$$\dot{a} = (Q'/18\pi)^{1/3} t^{-2/3} \tag{2.3}$$

and thus, by continuity,

$$\mathbf{u}(r,t) = \dot{a}a^2\hat{\mathbf{r}}/r^2 = Q'\hat{\mathbf{r}}/(2\pi r^2), \tag{2.4a, b}$$

where r is a radial co-ordinate and $\hat{\mathbf{r}}$ the unit vector in the radial direction. Hence, by integration of (1.1)

$$p = \mu a^2 \dot{a}/(kr) + p_0 \tag{2.5a}$$

$$= \frac{1}{2\pi}\mu Q'/(kr) + p_0, \tag{2.5b}$$

independent of time, where p_0 is a constant reference pressure.

In the gravity current regime, the following relationships have been determined (Lyle et al. 2006).

$$r_N(t) = 1.16(\beta Q')^{1/4} t^{1/2} \tag{2.6}$$

$$h(r,t) = (Q'/\beta)^{1/2}\Phi[r/r_N(t)] \tag{2.7a}$$

$$\approx 0.67(Q'/\beta)^{1/2}(1 - r/r_N), \tag{2.7b}$$

for some function $\Phi(y)$, which does not have a closed form, analytical solution and $\beta = \Delta\rho g k/(\phi\mu)$.

Actually, $h(r,t)$, as determined by similarity theory, has a logarithmic singularity at $r = 0$ and so $h(0,t)$ is infinite (for the similarity solution). However, away from $r = 0$ the shape is so well represented by the linear representation of (2.7b) that we write

$$h(0,t) = 0.67(Q'/\beta)^{1/2}. \tag{2.8}$$

The accuracy of this expression can be seen from the fact that

$$\frac{1}{3}\pi r_N^2 h(0,t) = 0.94Q't \tag{2.9}$$

rather than the correct value of $Q't$. Thus using (2.6), we can write

$$\gamma(t) = 0.58(Q'/\beta^3)^{1/4} t^{-1/2}. \tag{2.10}$$

In terms of the time and length scales

$$T = (Q'/\beta^3)^{1/2} \quad \text{and} \quad L = (Q'/\beta)^{1/2}, \tag{2.11a, b}$$

both of which are increasing functions of each of the flux rate and dynamic viscosity, and decreasing functions of each of the permeability and density difference between intruding and intruded fluid, these become

$$a/L = (3/2\pi)^{1/3}(t/T)^{1/3} \tag{2.12}$$

$$r_N/L = 1.16(t/T)^{1/2} \tag{2.13}$$

$$h(0,t)/L = 0.67 \tag{2.14}$$

and

$$\gamma = 0.58(t/T)^{-1/2}. \tag{2.15}$$

We define $A(t)$ as the ratio of the effects of gravity, $\Delta\rho g$, to the effects of flow, $\mu u/k$,

where u is a suitable velocity, and therefore

$$A(t) = k\Delta\rho g/(\mu u). \tag{2.16}$$

Substituting $u(a,t)$ from (2.4), we determine the value of the Alison number for the first period of the flow, $A_1(t)$, as

$$\begin{aligned} A_1(t) &= 2\pi(\beta\phi/\phi')a^2 && (2.17a)\\ &= (18\pi)^{1/3}\beta\phi Q'^{-1/3}t^{2/3} && (2.17b)\\ &= 18\pi^{1/3}\phi(t/T)^{2/3}. && (2.17c) \end{aligned}$$

For the second period, the effective u is given, in order of magnitude, from (2.6) by

$$\begin{aligned} u &= 0.58(\beta Q')^{1/4}t^{-1/2} && (2.18a)\\ &= 0.58LT^{-1}(t/T)^{1/2} && (2.18b) \end{aligned}$$

and so

$$\begin{aligned} A_2(t) &= 1.72(\beta^3/a')^{1/4}t^{1/2} && (2.19a)\\ &= 1.72\phi(t/T)^{1/2}, && (2.19b) \end{aligned}$$

suggesting that the time of transition, t_A, between the first and second period, as far as the Alison number is concerned, is given by ($A_1 = A_2$)

$$t_A/T = 0.0081 \tag{2.20}$$

at which time

$$a/L = h/L = 0.157 \tag{2.21}$$

and therefore gravity begins to become important at less than one hundredth of the timescale T with a transition that occurs well before $A_2 = 1$.

Alternatively, a different time for transition, t_a, may be defined by $a = r_N$ which is given by

$$t_a/T = 0.0936, \tag{2.22}$$

with

$$a/L = h/L = 0.355, \tag{2.23}$$

indicating the flow begins to look like a gravity current after less than one tenth of T.

Additionally, we could consider the transition time, t_γ defined by $\gamma(t_\gamma) = 1$, where γ is given by the expression valid in the second gravity current regime (2.6) and (2.8), which leads to

$$t_\gamma/T = 0.336, \tag{2.24}$$

at which time

$$a/L = R/L = 0.543. \tag{2.25}$$

Graphs of $A(t)/\phi, h/Lr_N/L$ and γ are presented in figure 2, wherein somewhat surprisingly, $t_\gamma < t_h$. Finally, we can evaluate the time t_h at which the height over the input takes the same value in the relationships for the two different phases as

$$t_h/T = 0.629, \tag{2.26}$$

at which time

$$r_N/L = 0.92 \quad \text{and} \quad h/L = 0.67. \tag{2.27a, b}$$

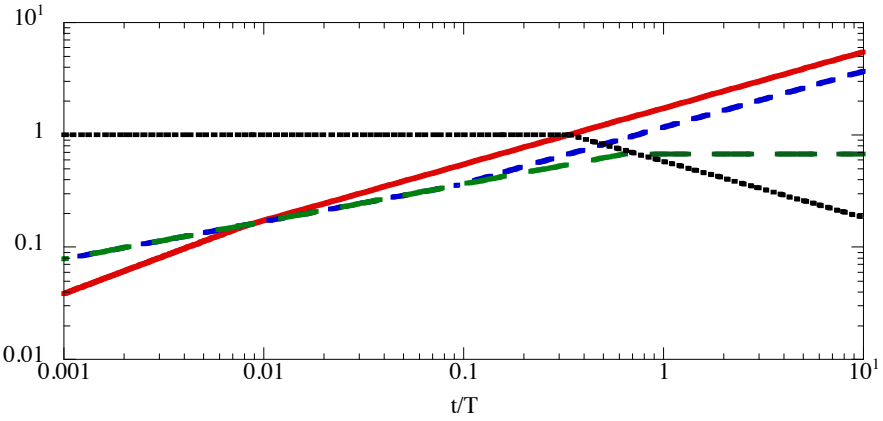

FIGURE 2. $A/\phi, r_N(t), h(0,t)$ and $\gamma(t) = h(0,t)/r_N$ for the initial and final responses in an axisymmetric situation. The points where the curves meet are depicted.

3. A Hele-Shaw cell

The consideration of a thin Hele-Shaw cell (Batchelor 2000, Huppert 1986 and Huppert & Wooods 1995) leads to a very similar exposition, though quantitatively different from the axisymmtric situation. The description will hence be brief.

In the initial stages, when gravitational effects are irrelevant, conservation of volume dicates

$$\frac{1}{2}\pi a^2 = F' t, \tag{3.1}$$

where F is the constant two-dimensional input rate and $F' = F/\phi$. With length and time scales of

$$L_2 = F'/\beta \quad \text{and} \quad \mathrm{T}_2 = \mathrm{F}'/\beta^2 \tag{3.2a, b}$$

(3.1) becomes

$$a(t)/L_2 = (2/\pi)^{1/2}(t/T_2)^{1/2}. \tag{3.3}$$

Using (4.14), (4.15) and (4.17) of Huppert (1986) and (3.13) of Huppert & Woods (1995), we can write for the second period, when gravity dominates,

$$x_N(t)/L_2 = 1.48(t/T_2)^{2/3} \quad \text{and} \tag{3.4a}$$
$$h(0,t)/L_2 = 1.46(t/T_2)^{1/3} \quad \text{so that} \tag{3.4b}$$
$$\gamma = 1.01(t/T)^{1/3}. \tag{3.4c}$$

Thus

$$A_1(t) = (2\pi)^{1/2}\phi(t/T_2)^{1/2} \quad \text{and} \tag{3.5a}$$
$$A_2(t) = 1.01\phi(t/T_2)^{1/3}. \tag{3.5b}$$

Proceeding as before, we determine that

$$t_A/T_2 = 0.00428,\ t_a/T_2 = 0.0246,\ t_\gamma/T_2 = 1.03,\ t_h/T_2 = 37.5. \tag{3.6a, b}$$

We note the considerably wider range of these changes over time in comparison to their axisymmetric counterparts.

Figure 3 presents the curves outlined in (3.3)-(3.5). We see that qualitatively the results

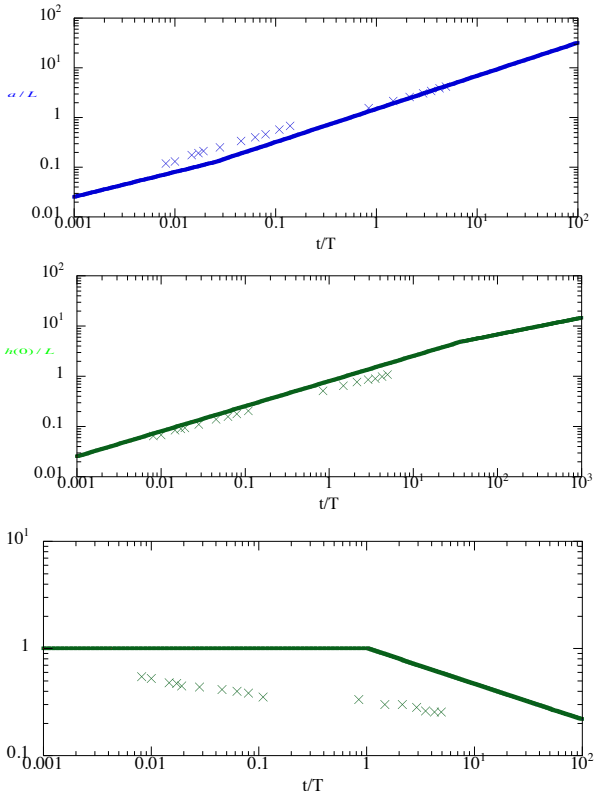

FIGURE 3. The two-dimensional experimental data compared with the two asymptotic curves for a) A/ϕ, b)r_N and c) h and d, γ.

for the axisymmetric and two-dimensional geometries are similar, though quantitatively they are quite different.

4. Numerical values

To get a feel for the various time scales, we present numerical values in tables 1 and 2 using typical laboratory and geological values. The time scales in the laboratory are, unsurprisingly, much less than those in the Earth. However, those for the laboratory are so short that the first regime would typically be a very small, initial part of any experiment, partially influenced by details of the input conditions, such as the radius of the input conduit [HEH include a, h @ various t/T?] However, those in the Earth, for realistic values, vary considerably, over many orders of magnitude. For the larger ones, other processes can occur such as chemical reactions with the surrounding rocks that can either increase or decrease permeability, as well as crystallization of the magma or even complete solidification. Extensions to our first-step model would then be needed; and will be preserved in the future elsewhere.

5. Experimental analysis

We conducted a series of laboratory experiments in an effectively two-dimensional acrylic tank of length 200 cm, height 25 cm and width 1 cm, as illustrated in figure 4.

T(s)	$T(yr)$	t_A	t_a	t_r	t_h
5.00e+10	1580	12.8	148	532	996
1.58e+11	5010	40.6	469	1680	3150
2.74e+12	86780	703	8120	29200	54600
7.91e+06	0.25	0.00203	0.023	0.084	0.158
2.50e+07	0.79	0.00642	0.074	0.266	0.498
4.33e+08	13.7	0.111	1.280	4.610	8.631
1.00	1.00	0.00810	0.094	0.336	0.629

TABLE 1. The various time scales for axisymmetric flows, in years, except for the last two lines, 3a,b, which is in seconds, for the following cases with $\Delta\rho/\rho = 0.01, g = 10m^1s^{-2}$ and $\nu = 10^{-6}m^3s^{-1}$. 1 $\phi = 0.05, k = 10^{-15}m^2$, for which $\beta = 2 \times 10^{-9}ms^{-1}$. 2 $\phi = 0.25, k = 10^{-12}m^2$, for which $\beta = 4 \times 10^{-7}ms^{-1}$. A : $Q = 10^{-6}m^3s^{-1}$. B : $Q = 10^{-5}m^3s^{-1}$. C : $Q = 3 \times 10^{-3}m^3s^{-1}$. 3. $\phi = 0.4, k = 2 \times 10^{-3}cm^2$ for which $\beta = 5cms^{-1} Q = 50cm^3s^{-1}$

.

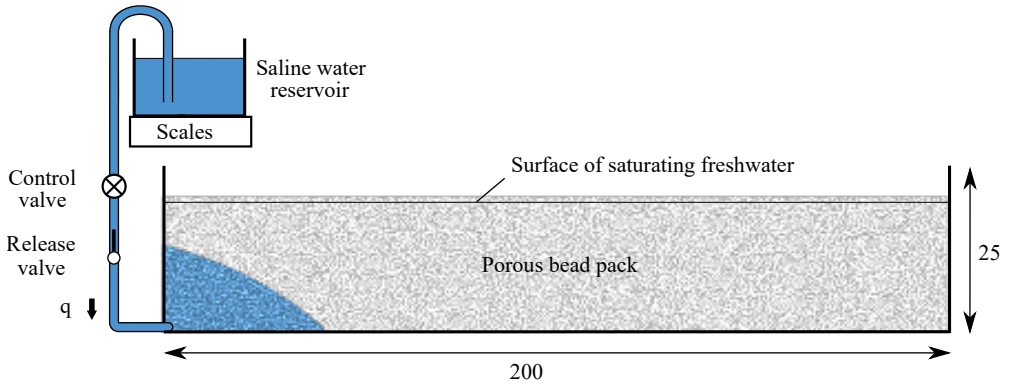

FIGURE 4. Schematic of our experimental apparatus.

The tank was filled with glass beads of diameter 2 mm, creating a porous medium of porosity $\phi \approx 0.39$ and permeability $k \approx 3.1 \times 10^{-5}$ cm^{-2}. The medium was saturated with freshwater of density 0.999 g cm^{-3}. Solutions of dyed and slightly salty water of densities varying from 1.011 to 1.035 g cm^{-3} between experiments, and kinematic viscosity $\nu \approx 0.010$ cm^2 s^{-1}, measured using an oscillating U-tube density meter and a U-tube viscometer respectively, were introduced into the medium through an inlet located at the bottom left-hand corner of the cell. The inlet was connected by a syphon of rubber tubing to a raised reservoir of salty water; the release of fluid was initiated using an intermediary ball valve. The evolution of the flow was recorded using a digital SLR camera, which took photographs once every second. The rate of input was determined by measuring the weight of the reservoir over the course of each experiment.

The parameter values used for five well-constrained experiments are shown in table 2. The main parameter varied was the volumetric rate of input per unit width Q, which spanned an order of magnitude from 0.2 to 2 cm^2 s^{-1}. The evolutions of the scaled frontal position and ratio of the height of the current to its length, as measured digitally from the photographs, are shown in figure 5a,b. Figure 5c plots γ, the ratio of the height of the current above the source to its horizontal extent. Overlaid are the early- and late-time predictions of (3.3) and (3.4). The data indicates that each experiment undergoes

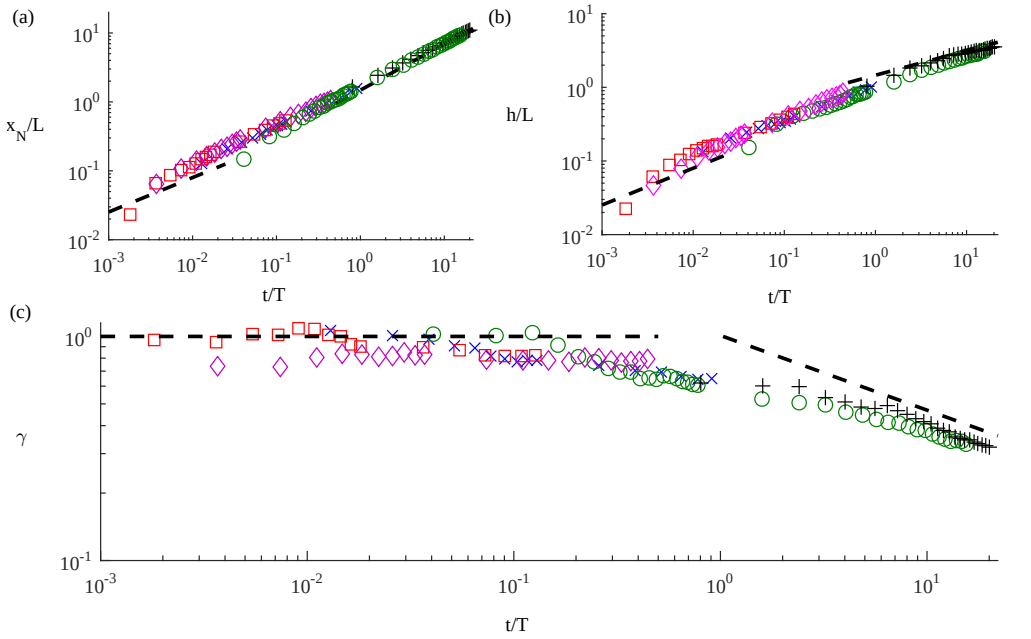

FIGURE 5. Experimental data showing (a) the horizontal length of the current scaled by the length scale L defined by (2.11b), (b) the height above the input point scaled by L and (c) the aspect ratio of the current γ (height over length) as functions of dimensionless time t/T, where T is the time scale (2.11a); the symbols denoting each experiment are given in table 2. The early-time predictions for x_N/L and γ associated with the radial regime (3.3), and late-time predictions associated with gravity-current regime (3.4) are shown as dashed lines.

Experiment	Q (cm^2 s^{-1})	$\Delta\rho$ (g cm^{-3})
1 (×)	2.15	0.036
2 (○)	0.68	0.036
3 (□)	1.83	0.012
4 (◇)	0.90	0.012
5 (+)	0.21	0.012

TABLE 2. Parameter values used in the experiments.

a transition from a regime of radial flow to that of the gravity current, with the various experiments spanning different intervals of the theoretical transition. Some early-time scatter of the aspect ratio shown in figure 5b is likely caused by the sensitivity of the early-time flow to some inhomogeneities in the permeability of the bead pack.

6. Vertically varying permeability and porosity

In the Earth there can be considerable variations in permeability and porosity in both vertical and horizontal directions. Considering only vertical variations, we realise that it may be possible for an expansion in the approximately hemispherical phase to intrude into a region where the expansion can proceed more like a gravity current. A sketch of this response in a two-layer system (with a much more permeable upper layer) makes up figure 6.

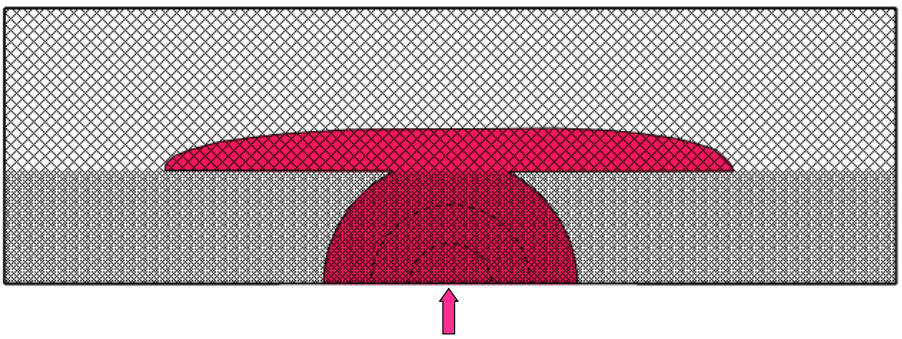

FIGURE 6. The typical response in a one-layer system shown in fig. 1 is compared with the possible response in a two-layer system.

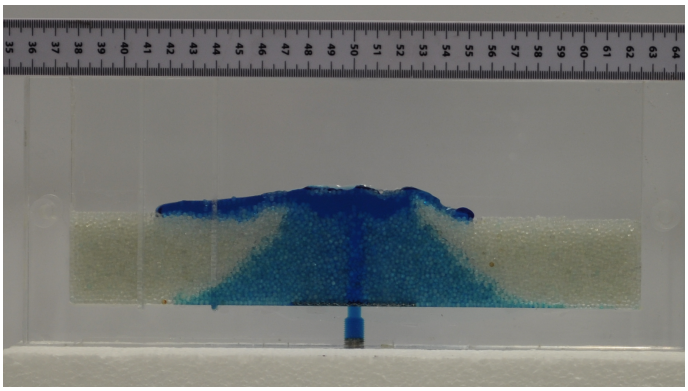

FIGURE 7. The result of an experiment in a porous layer through which the fluid penetrates the air above and flows along the top of the layer as a gravity current. There is an online movie of this whole experimental situation also.

To confirm this form of response in the laboratory, we carried out an experiment in the extreme case of a porous layer topped by air in a Hele Shaw cell of width 10mm filled with glass ballotini of diameter 2mm to a depth of 4cm. An input of blue-dyed glycerine of viscosity $7.5\text{cm}^2 s^{-1}$ and density 1.26gm cm^{-3} was fed at a rate of $0.18\text{cm}^2 s^{-1}$ to the base of the container and photos taken every 2s. A movie of the experiment makes up online 1. There was the roughly semi-circular spreading, as expected, until after approximately 100s the flow was effectively at the top of the layer, though there was some vertical uplift of the beads as the flow approached the interface. By 140s there was a clearly evident horizontal flow along the interface with lengthens with time. Parts of the heavy fluid sunk back into the porous layer in the form of broad fingers, replicating the motions first seen by Acton, Huppert & Worster (2001).

7. Summary

We have evaluated, theoretically and experimentally, the response to the constant injection at a point source of a viscous fluid relatively more dense than the interstitial fluid of the surrounding porous medium. The porous medium lies above a rigid horizontal boundary and the source point is at that boundary. The analysis was presented both for an axisymmetric, radial expansion and for the two-dimensional situation. We show that the fluid expands first hemisperically (in a semi-disc in the two-dimensional situation),

where gravitational effects are negligible, and then transitions to a small slope gravity current.

We evaluate the only time scale, T say, in the problem and show that there is a wide range of different transition times, dependent on which of a series of different quantities are used to define the transition time as given by the equality of the quantities evaluated in the two different extreme regimes.

Considering the ratio between viscous and gravitational forces, which we call the Alison number [($A(t)$, where t is time], we find, for the fully three-dimensional, axisymmetric case, that the transition time $t_A/T = 0.0081$ (0.00428 for the two-dimensional situation).

Considering the horizontal radius of the resulting flow, we evaluated the transition time $t_r = 0.0936$ for axisymmetric situations (and 0.0246 for the two-dimensional situation). Considering the height of the flow above the source point, we find that $t_h/T = 0.629$ (37.5 for two-dimensional situations); while considering a slope, defined by the ratio of height above the input to the horizontal radius at the boundary, the ratio of the two previous criteria, $t_\gamma/T = 0.336$ (1.03 for two-dimensional situations). This large difference between the various time scales – almost 80 in the axisymmetric situation (approximately 8760 for the two-dimensional situation) – is somewhat surprising. It shows that different aspects of the flow become important at different times.

Because the overall timescale T is quite strongly dependent on the permeability – to the minus three halves in the axisymmetric situation (and inversely proportional in the two-dimensional situation) – it suggests that a lower, relatively impermeable, layer may display a roughly hemispherical (disc like in two-dimensions) shape while at the same time an upper much more permeable layer, at which fluid arrived later, could already be well into the gravity current regime. Such a situation makes up figures 6 and 7 (and has already been demonstrated by experiment in numerous places around the world during seminars by one of us - HEH). There are similarities to the configuration analysed theoretically and experimentally by Huppert et al. (2013) who determined what conditions an input of relatively heavy fluid into the base of a two-layered porous medium flows into the upper layer because of its greater permeability.

In the current situation, because the timescale depends on parameters whose value is very different in illustrative laboratory settings and in the Earth, the relatively rapid transition to a gravity current – taking seconds at most in the laboratory, can take thousands of years in the Earth.

There are also similarities with the study of Pegler et al. (2013) who model the movement of ice across land into water, departing from the solid ground at the grounding line, by introducing a viscous gravity current at the surface of a relatively more dense and much less viscous fluid layer of finite depth. The flow undergoes a transition from a radial flow driven predominantly by the pressure gradient towards a buoyancy-driven regime of predominantly horizontal flow. They evaluate the transition radius, which they call $\Re$ and present a graph (figure 6) of the experimental data compared with the theoretical result, with reasonable agreement, for the time T at which the transition occurs.

We thank Mark Hallworth who helped with the experiment described in §6. HEH is grateful for support in the form of a Leverhulme Emeritus Fellowship. The research of RSJS is partially supported by the European Research Council in the VOLDIES project. Any other acknowledgements needed?

REFERENCES

Acton, J.M., Huppert, H.E. & Worster, M.G. 2001 Two-dimensional viscous gravity currents flowing over a deep porous medium. *J. Fluid Mech.* **440**, 359-380.

Batchelor, G.K. 2000 An Introduction to Fluid Dynamics Cambridge University Press.

Bear, J. 1972 Dynamics of Fluids in Porous Media New York. Dover.

Bickle, M.J. 2009 Carbon storage. *Nat. Geosci.* **2**, 815-818.

Huppert, H.E. 1986 The intrusion of fluid mechanics into geology. *J. Fluid Mech.* **173**, 557-594.

Huppert, H.E. & Neufeld, J.A. 2014 The fluid mechanics of carbon dioxide sequestration. *Annu. Rev. Fluid Mech.* **46**, 255-272.

Huppert, H.E., Neufeld, J.A. & Strandkvist, C. 2013 The competition between gravity and flow focusing in two-layered porous media. *J. Fluid Mech.* **720**, 5-14.

Huppert, H.E. & Woods, A.W. 1995 Gravity-driven flows in porous layers. *J. Fluid Mech.* **292**, 55-69.

Morton, B.R., Taylor, G.I. & Turner, S. 1956 Turbulent gravitational convection from maintained and instantaneous sources. *Proc. Roy. Soc.* **234A**, 1-23.

Pegler, S.S., Kowal, K.N., Hasenclever, L.Q. & Worster, M.G. 2013 Lateral controls on grounding-line dynamics. *J. Fluid Mech.* **722**.

Phillips, O.M. 1991 Geological Fluid Mechanics: Sub-surface Flow and Reactions. Cambridge University Press.

Simpson, J.E. 1987 Gravity currents in the Environment and the Laboratory. Cambridge University Press.

Turner, J.S. 1973 Buoyancy Effects in Fluids. Cambridge University Press.

Turner, J.S. 1986 Turbulent entrainment: the development of the entrainment assumption, and its application to geophysical flows. *J. Fluid Mech.* **173**, 431-471.

Ungarish, M. 2009 An Introduction to Gravity Currents and Intrusions. CRC Press.